FILOMAT (Niš) 9:2 (1995), 207–231
Filomat '94, Niš, October 22-24, 1994
Geometry. Computer Sciences

FRACTALS AND THEIR APPLICATIONS IN COMPUTER GRAPHICS

Ljubiša M. Kocić

ABSTRACT. *The paper presents elements of fractal geometry and its application in computer graphics and geometric modeling. A connection with chaos dynamics, mostly from historical angle of view, is stressed. Two fundamental algorithms for computing fractal attractors are described. Barnsley affine iterated function systems (IFS) are described as means of constructing deterministic fractals. It is pointed out how to introduce parameters in IFS, via Bernstein polynomials, to produce different natural forms. Variety of applications: in animation, data compressing, rendering objects and modeling phenomena in physics and biology are described.*

1. Introduction: Physics and History

At the end of 19. century, physicists considered Physics as a mainly finished discipline, with everything of any importance in the field being already explained and known. Everything, except a couple of unimportant loose ends. Making efforts to remove them, Schrödinger discovered quantum mechanics, while Einstein invented the relativity theory. The new physics required new mathematical techniques, and before all, new geometry. So, the non-euclidean and projective geometries became topics of interest. Just when it seemed that relativity theory would finally finish the job of completing the great book of nature being opened by the Newton physics, the strange properties of simple oscillators have been noticed. Actually, under certain circumstances, they began to exhibit irregular, chaotic behaviour. Thus, in the last quarter of 20-th century, scientists have faced the new revolution called *chaos*.

1991 *Mathematics Subject Classification.* 58F13.
Key words and phrases. Fractal sets, chaos, computer graphics.
This research was partly supported by Science Fund of Serbia, grant number 0401A, through Matematički institut

The word 'chaos' ($\chi\alpha o\varsigma$) stems from the old Greek *hainō* which means 'open widely'. In Aristotel's works, 'chaos' is used to denote an 'empty space'. Later, in the history, this word becomes the synonym for 'mess' and 'lack of order'.

Chaos cannot be successfully described neither by Euclid geometry nor by non-euclidean or projective geometries. Except in some crystal forms, nature rarely exhibits regularity and geometric order. Natural forms and structures are irregular and chaotic: clouds, moss, trees, coastlines, feathers, rocks, surface of the sea, network of neurons etc. These are forms that *fractal geometry* deals with.

Phenomenology of chaos appears in, at least three planes. The plane of *morphology* is the most accessible for studying due to huge amount the empirical, factual material which is collected during the time. The plane of *logic* is much more complicated, so that only the partial breakthrough has been done (for ex. in information theory). The *causality* plane is still in domain of hypothesis and till now, it is beyond the experimental confirmation. Typical example is the hypothetical 'quantum chaos'.

Much earlier before the physicists started coping with chaos, there were hints of it in mathematical thinking.

So, at the beginning of 19. century Laplace introduced the new discipline to describe unruliness and disorder – *probability theory*. Contrary to deterministic theories, probability theory states that future depends randomly on the past.

Then, Weierstrass defined the function

$$f(x) = \sum_{i=1}^{\infty} \frac{\sin(\lambda^i x)}{\lambda^{\varepsilon i}} \ , \ x \in [0, 2\pi] \ ,$$

where $\lambda > 1$ and $0 < \varepsilon < 1$ are real parameters. Being continuous but nowhere differentiable [12 , p. 53], this function was unlike the things that mathematicians had ever seen before. Although bounded, its graph has infinite length (Figure 1-a).

Actually, Weierstrass function belongs to the 'fractal' class $\mathbf{C}^{\varepsilon}$. *Topological dimension* of this curve is $\mathrm{Dim}_T = 1$, while its *Hausdorff* (also called *Hausdorff–Besicovitch* or *geometric*, see Section 4.) dimension is apparently $\mathrm{Dim}_H = 2 - \varepsilon$, but this has not been proved rigorously [15].

The most famous fractal set is probably the Cantor set which is equipotent to the interval $[0, 1]$ but of zero measure. Its Hausdorff dimension is $\mathrm{Dim}_H = \ln 2 / \ln 3 = 0.6309...$ and topological dimension $\mathrm{Dim}_T = 0$ (Fig. 1-b). So, the Cantor set can not be reduced to a set of isolated points in which case its H-dimension should be $\mathrm{Dim}_H = 0$.

Figure 1. a) The Weierstrass function for $\lambda = 1.9$, $\varepsilon = 0.3$; b) Generating of the Cantor set

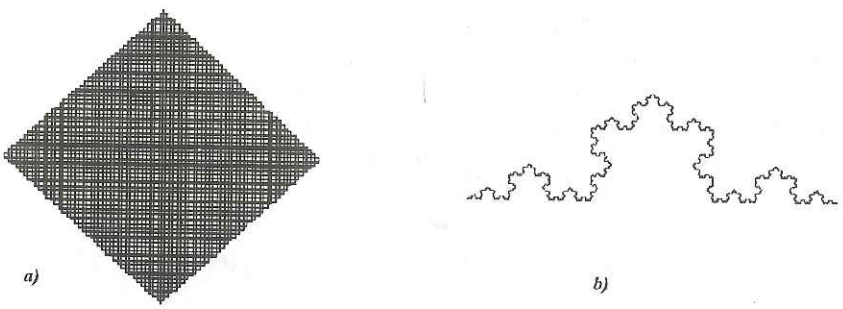

Figure 2. a) Peano curve; b) von Koch curve

In 1890. Peano [24] published a construction of a curve that fills in the unit square without self-intersections. *Peano* curve has Hausdorff dimension $\mathrm{Dim}_H = 2$, while $\mathrm{Dim}_T = 1$ (Figure 2-a). A year later, Hilbert [16] announced its own construction of such, so called *space filling curve.*

The next important construction is the von Koch curve from 1904 ([19]), known from calculus textbooks as an example of a simple continuous curve without tangents. Its geometrical dimension is $\mathrm{Dim}_H = \ln 4 / \ln 3 = 1.2619\ldots$, ($\mathrm{Dim}_T = 1$), see Figure 2-b.

These 'early birds' were named 'monsters' and 'pathological cases' by other mathematicians, and they refused to deal with them at all. In spite of lacking the tools (like modern computers), first systematic study of chaos

and irregular structures starts with works of Kowalewska and continues with works of Lyapunov.

Making efforts to describe the chaotic phenomena as accurate as it is possible, Poincaré introduces *topology* and considers the physical chaos on model of *orbits* of mapping $f : \mathbf{X} \to \mathbf{X}$:

$$x, \quad f(x) \quad f^2(x) \quad \dots , \quad x \in \mathbf{X} ,$$

and intersection of dynamic trajectory in m-dimensional *phase space* and transversal $(m-1)$-dimensional hyperplane, now known as the *Poincaré section.*

The ideas of Poincaré have been further developed by Gaston Julia and Pierre Fatou during 20-ies of this century. Their work drew attention of physicists due to its applicability to the simple dynamical systems called *oscillators.* A typical model is a pendulum, but there were other interesting oscillators.

So, B. van der Pol in Holland studied the oscillating model of an electronic tube, while the mathematician V. Arnold made detailed analysis of the mathematical model of the human heart, which is an oscillator by himself.

In 1950–es, ecologists have studied so called logistic equation which describes variations in population of different zoological forms

$$x_{n+1} = r\, x_n(1 - x_n) , \quad n \in N , \quad x_1 \in \mathbf{R} , \tag{1}$$

where $r \in \mathbf{R}$ is a parameter. The Sequence $\{x_n\}$ represents the orbit of a simple quadratic map

$$f : \; x \mapsto r\, x(1-x) , \quad r \in \mathbf{R} ,$$

which exhibits unexpected dynamical properties. For $r < 3$ the corresponding dynamical system $(f, \mathbf{R})$ is stable, ie. f is a contractive mapping with a unique fixed point $x = lim_{n \to +\infty} x_n$. For $3 < r < 3.5699456\dots$, the system has periodical behaviour with successively doubling of the period, whilst for the bigger values of r it goes to chaos. The graph of x as function of r is known as *bifurcation diagram* The sequence of branching points (bifurcations) $\{r_n\}$ has an accumulating point $3.5699456\dots$, which marks the limit of stability. The ratio $\Delta r_n / \Delta r_{n+1} = 4.6692016091\dots$ is invariant for all mappings with 'parabolic' maximum and is referred as the *Figenbaum number.*

This type of mapping describes 'explosions' in biological population like the famous locust flood every seven years, unexpected starting and spreading

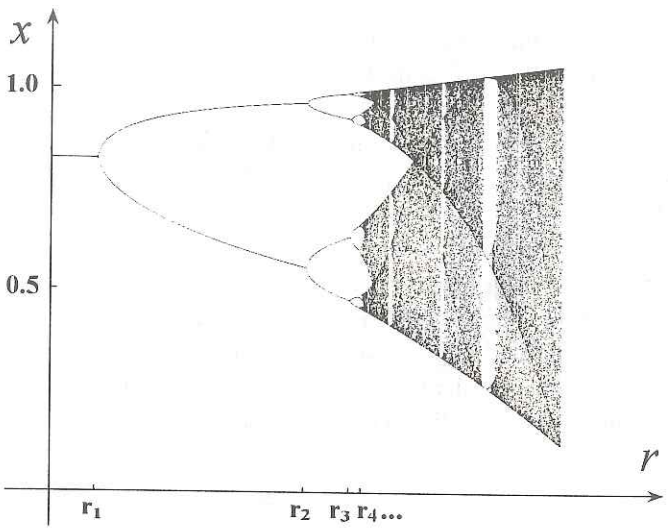

Figure 3. The bifurcation diagram for logistic equation.

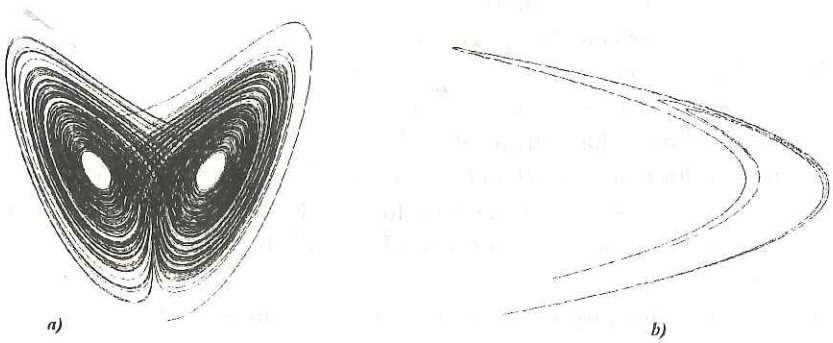

Figure 4. a) Lorentz attractor; b) Hénon attractor

of diseases, but it also describes fluctuation of the money value on the market, where chaos means the economical breakdown.

In 1962., Edward Lorenz made a mathematical model of meteorological variations of weather, being described by the set of differential equations

$$(2) \qquad x'(t) = a(y - x)\ ,\quad y'(t) = bx - y - xz\ ,\quad z'(t) = xy - cz\ ,$$

in time domain. It comes out that the model gives good results, but it is very sensitive on initial conditions for some parameter values. It implies its sensitivity
on the error which is accumulated during the numerical integration process. The exact solution of (2) is a trajectory in $\mathbf{R}^3$ which has very complicated form. (For its XY-projection, see Figure 4-a). If converging, the numerical solution approaches (in the Hausdorff metric) this trajectory, the reason led Lorenz in name it *strange attractor*. In 1963., Michelle Hénon, a French astronomer, used Poincaré's ideas and include chaos in mechanical model of stars motion. This helped him to overcome a many years standstill in the problem, caused by the classical newtonian approach. The Hénon model can be reduced to the system of difference equations

$$x_{n+1} = 1 - \alpha x_n^2 + y_n \ , \ y_{n+1} = \beta x_n \ ,$$

whose attractor, for $\alpha = 1.4$ and $\beta = 0.3$ has a remarkable self–similar '3–2–1 pattern' structure (Figure 4-b).

2. Deterministic fractals

Two important observations lead to the fractal geometry.

1° The Nature is permeated with something that scientists call *deterministic chaos*. This is the common name of the behaviour of the huge number of fairly simple physical systems that are governed by deterministic law, but, in spite of this, they behave unpredictably.

2° There is a *hierarchical structure* in the Universe. Details resembles to the whole: it can be easily noticed in forms of crystals and plants, in the relief of Earth surface, in the structure of stellar clusters and in variation of market prices.

During sixties, the physics of chaos becomes more and more attractive field. The remarkable oscillatory chemical reaction of *Belousov-Žabotinski* is explained by using chaos. It was discovered that there are three 'scenarios' for a system to pass to chaos. These types can be described by purely geometrical language, depending on the type of bifurcation of dynamical system.

In seventies, Benoit Mandelbrot from IBM-a, made, by the help of computer, first fractal images. These are graphical 'portraits' of dynamics of simple mappings with astonishing degree of disorder, but this disorder was systematic and unusually complex. The most popular among these pictures is probably the *Mandelbrot set* (Figure 5). It represents the dynamical chart of mapping $z \to z^2 + C$, $z \in \mathbf{C}$, for fixed value of complex constant C. Orbits are given by the sequence $\{z_n\}$, which is the solution of difference equation

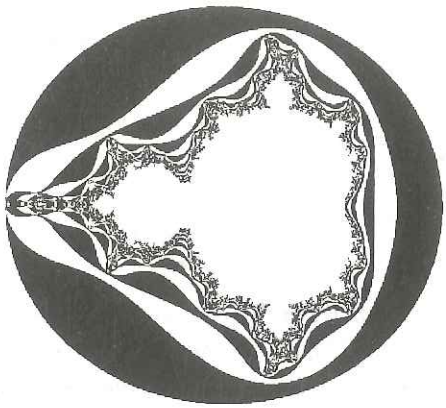

Figure 5. The Mandelbrot set.

$z_{n+1} = z_n^2 + C$, $z_0 = 0$. For a given value C, the behaviour of sequence $\{z_n\}$ has been examined. If it diverges, the point C in the complex plane are 'painted' in, for ex., black color. If converges, it will be painted in some lighter color, as lighter as faster the convergence is (in Fig. 5, this is white). The Mandelbrot set has an important role in fractal geometry, as for ex., circle in Euclid's geometry, and it is studied out exhaustively [5].

Mandelbrot coined the word "fractal" from lat. *fractus* which means a stone, broken and having irregular form. In collaboration with other scientists, he studies a large variety of phenomena being connected with fractals: stochastic form of a coastline and its relationship with Brownian motion, turbulence in fluids, statistical distribution of telephone calls, Nile floodings, branching neurons in the neural tissue etc. By the way, Mandelbrot noticed that fractal images possess aesthetical values.

In 1982. the fundamental Mandelbrot book [22] appeared. The new discipline was born. It includes fractal geometry as its most important part. After the book has been issued, the interest on fractal exploded. Many definitions of fractal sets and their dimensions appeared ([5],[7],[8], [11],[13],[15],[30]).

In this section, a large class of fractal sets will be introduced. This very class has application in computer graphics in modeling natural phenomena.

The notation $(\mathbf{X}, d)$ throughout the text will denote the complete metric space. Also, $\mathcal{H}(\mathbf{X})$ will denote the space whose points are compact subsets of $\mathbf{X}$.

Definition 1. A map $F : \mathbf{X} \to \mathbf{X}$ of a metric space $(\mathbf{X}, d)$ is a *Lipschitz map* if there is a number σ such that $d(F(x), F(y)) \leq \sigma d(x, y)$, for all $x, y \in \mathbf{X}$.

The least such number, $s(F) = \min\{\sigma\}$ is the *Lipschitz constant* of F. If $s(F) < 1$ then F is called a *contraction*.

Definition 2. Let '$\circ$' be a usual composition of mappings. Then, $F^{\circ n}$ denotes n-th iteration of a mapping F, i.e.

$$F^{\circ n} = F(F^{\circ(n-1)}) \ , \quad F^1 = F \ .$$

Theorem 1 (Contraction principle). *If F is a contraction $\mathbf{X} \to \mathbf{X}$, then the sequence $\{n \mapsto F^{\circ n}(x)\}_{n=0}^{+\infty}$ converges to a fixed point $a \in \mathbf{X}$ of F. The fixed point is unique. Moreover, if s is the Lipschitz constant of F, then*

$$d(F^{\circ n}(x), a) \leq \frac{s^n}{1-s} d(F(x), x) \ .$$

Proof. For the proof, see any textbook in functional analysis. □

Definition 3. For any $x \in \mathbf{X}$ and $B \in \mathcal{H}(\mathbf{X})$, the distance from the point x to the set B is

$$d(x, B) = \min_{b \in B}\{d(x, b)\} \ .$$

Definition 4. For any $A, B \in \mathcal{H}(\mathbf{X})$, the distance from A to B is

$$\rho(A, B) = \max_{x \in A}\{d(x, B)\} \ .$$

It is easy to see that ρ is not symmetric, i.e. $\rho(A, B) \neq \rho(B, A)$, so ρ does not provide a metric on $\mathcal{H}(\mathbf{X})$.

Definition 5. For any $A, B \in \mathcal{H}(\mathbf{X})$, the Hausdorff distance between A and B (induced by the metric d) is

$$h(A, B) = \max\{\rho(A, B), \rho(B, A)\} \ .$$

Theorem 2. *The Hausdorff distance h is a metric on the space $\mathcal{H}(\mathbf{X})$. The space $(\mathcal{H}(\mathbf{X}), h)$ is a complete metric space.*

Proof. See [1]. □

Definition 6. *A (hyperbolic) function system* (IFS) is a set $S = \{\mathbf{X}; f_i\}_{i=1}^m$, where f_i is a contraction of $(\mathbf{X}, d)$ into itself. If s_i is a Lipschitz constant for f_i, then $s = \max_i\{s_i\}$ is the Lipschitz contractive constant for the IFS.

Theorem 3 (Hutchinson). *Let S, be an IFS, with contractive constant s. For $A \in \mathcal{H}(\mathbf{X})$, define $F(A) = \cup_{i=1}^{m} f_i(A)$. Then,*

$$h\{F(A),\ F(B)\} \leq sh(A,\ B)\ ,\ A, B \in \mathcal{H}(\mathbf{X})\ ,$$

Proof. See [17]. □

Definition 7. A set $A \in \mathcal{H}(\mathbf{X})$ is an attractor of IFS $\{\mathbf{X}, f_i, i = 1, \ldots m\}$ if $F(A) = A$. Sometimes attractors are called *deterministic fractals.*

Theorem 4 (Hutchinson). *There is a unique closed bounded attractor A for S. Moreover, if B is any set from $\mathcal{H}(\mathbf{X})$, then*

$$A = \lim_{n \to \infty} F^{\circ n} B\ .$$

Proof. See [17]. □

3. Algorithms, affine IFS and Bernstein polynomials

The fractal geometry is a discipline of computer ages. Without computers, exploration of fractal sets would not be possible. For the mutual benefit, fractals contribute in picture synthesis as an mighty tool. There are many algorithms for computing and visualizing fractals, but all are variations of two basic ones:

a) *Hutchinson's algorithm* [10]. This algorithm is based on Theorem 4. It starts from an initial set $B \in \mathbf{R}^2$ and transforms by the IFS recursively until graphical details become smaller than a pixel. This algorithm is also known as *deterministic algorithm.*

b) *Algorithm of Barnsley and Demko (random algorithm* [1],[2],[3]). It uses a positive sequence $\{p_i\}_{i=1}^{m}$ of probabilities so that $\sum p_i = 1$, where p_i is probability of application of contraction f_i in given iteration. Choose a point $x_0 \in \mathbf{X}$ and then, for $n = 1, 2, \ldots, m$, calculate

$$x_n = f_i(x_{n-1})\ ,$$

where index i is chosen randomly from $\{1, 2, \ldots, m\}$ with probability p_i. This procedure forms the sequence $\{x_n,\ n = 0, 1, \ldots\} \subset \mathbf{X}$ which approximates the attractor A of IFS. There are no precise rules for choosing the probabilities p_i, which allows flexibility in choosing the sequence $\{p_i\}$ which may be useful in modeling, as it will be shown in Section 4.

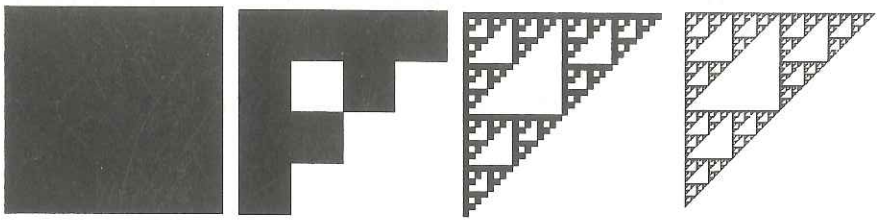

Figure 6. Four iterations of Hutchinson algorithm: Sierpinski gasket

An important class of deterministic fractals is defined by the IFS $\{\mathbf{R}^2; \phi_i\}$, (Euclidean metric), when ϕ_i are affine contractions, i.e.

$$\phi_i(\mathbf{x}) = \begin{bmatrix} a_i & b_i \\ c_i & d_i \end{bmatrix} \mathbf{x} + \begin{bmatrix} e_i \\ f_i \end{bmatrix} , \tag{3}$$

where $\mathbf{x} = [x \ y]^T \in \mathbf{R}^2$, and $a_i, b_i, c_i, d_i, e_i, f_i$ are real constants, chosen so that ϕ_i is a contraction. In this case, the probabilities p_i in Barnsley-Demko's algorithm can be calculated as

$$p_i = \frac{D_i}{\sum_{j=1}^{m} D_j} ,$$

where $D_i = |a_i c_i - b_i d_i|$ is the determinant of the matrix in (3).

It is hardly understandable how many different forms can be produced by an affine IFS. Let us see some examples.

1. *Sierpinski gasket.* It is a 'triangular extension' of Cantor set defined by the IFS $\{\mathbf{R}^2; \phi_1, \phi_2, \phi_3\}$, where $a_i = d_i = 0.5, b_i = 0, i = 1,2,3$, $c_1 = e_3 = 0.5$, $c_2 = c_3 = e_1 = f_1 = f_3 = 0$, $e_2 = 0.25$, $f_2 = \sqrt{3}/4$. Applying Hutchinson algorithm on the initial set–the unit square (leftmost in Figure 6), an approximation of the attractor is obtained through seven iterations (rightmost in Fig. 6). Figure 6 also shows third and fifth iteration. The same result will be obtained if any bounded initial set is taken. It is interesting that the Pascal triangle of binomial coefficients has fractal structure of Sierpinski triangle [31].

2. *Takagi function.* This is yet another fractal function that fits to the line of Weierstrass and von Koch construction. It was published in 1903 by Teiji Takagi [28]. It can be described by the affine IFS $(\mathbf{R}^2; \phi_1, \phi_2)$ so that

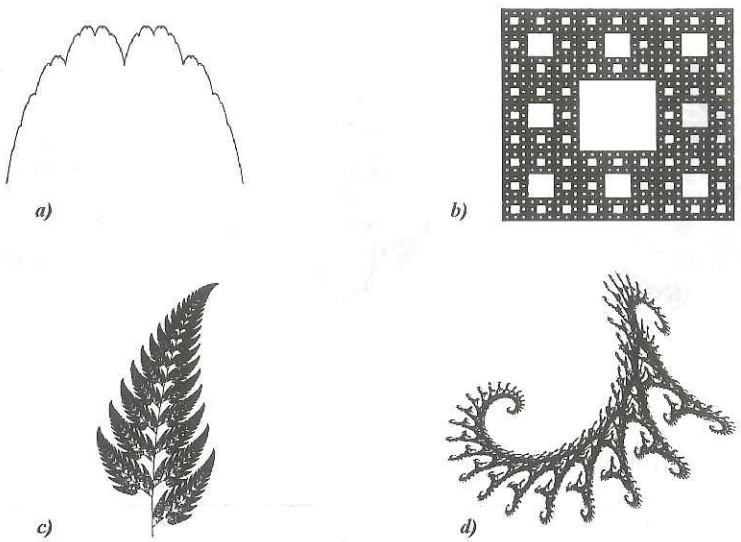

Figure 7. a) Takagi function; b) Sierpinski carpet; c) Barnsley fern; d) The dragon-like attractor

ϕ_1 and ϕ_2 are given by $a_1 = a_2 = c_1 = -c_2 = d_1 = d_2 = e_2 = f_2 = 0.5$, $b_1 = b_2 = e_1 = f_1 = 0$ with probabilities $p_1 = p_2 = 0.5$. The attractor, obtained by Barnsley-Demko algorithm is shown in Figure 7-a.

3. *Sierpinski carpet.* Yet another two-dimensional variation on Cantor theme. It is defined in $\mathbf{R}^2$ by eight affine transformations with coefficients: $a_1 = a_3 = a_6 = a_8 = -b_2 = b_4 = b_5 = -b_7 = c_2 = -c_4 = -c_5 = c_7 = d_1 = d_3 = d_6 = d_8 = e_2 = e_4 = e_5 = f_2 = f_5 = f_7 = 1/3$, $e_6 = e_8 = f_3 = f_8 = 2/3$, $e_7 = f_4 = 1$. Other entries are zero. The attractor is rendered by the random algorithm (Fig. 7-b).

4. *Barnsley fern.* An interesting fern-like attractor (Fig. 7-c) is found by M. Barnsley [1]. Four affine contractions are given by the coefficients

a	b	c	d	e	f	p
0.0	0.0	0	0.16	0.0	0.0	0.01
0.85	0.04	−0.04	0.85	0.0	1.6	0.85
0.2	−0.26	0.23	0.22	0.0	1.6	0.07
−0.15	0.28	0.26	0.24	0.0	0.44	0.07

The attractor, produced by random algorithm is shown in Figure 7-c.

5. *Dragon.* The dragon-like set (Fig. 7-d) is defined by IFS data

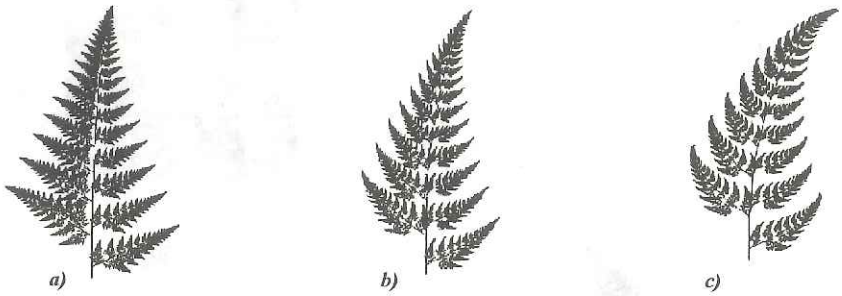

Figure 8. Wind in fractal plants: the parametric IFS

a	b	c	d	e	f	p
0.824074	0.281482	−0.212346	0.864198	−1.882290	−0.110607	0.787473
0.088272	0.520988	−0.463889	−0.377778	0.785360	8.095795	0.212527

It is of special importance to introduce one or several parameters into IFS, so that the form of attractor set depends on them. Parameters should be incorporated in such a way that affine mappings in IFS maintain their contractive properties for a whole range of parameter changing. Actually, the following theorem takes place.

Theorem 4 (Barnsley). *Let $(\mathbf{X}, d)$ be a metric space, and $\{\mathbf{X}; f_1, \ldots, f_N\}$ be a hyperbolic IFS of contractivity s. Let f_n depend continuously on a parameter $p \in P$, where P is a compact metric space. Then, the attractor $A(p) \in \mathcal{H}(\mathbf{X})$ depends continuously on $p \in P$, with respect to the Hausdorff metric $h(d)$.*

Proof. See [1]. □

This theorem provides a way of controlling the shape of IFS in continuous way. It can be used very effectively in modeling motion of fractal objects. For example, the fern swung by the wind may be obtained by simple changing a parameter in IFS-fern data so to get a plant without wind (Figure 8-a), under breeze (Fig. 8-b) and stronger wind (Fig. 8-c). Such effects are especially important in animation.

An elegant way to introduce parameters in iterated function systems is to put one-variable real functions as IFS coefficients in (3). Author made some experiments using cubic Bernstein polynomials

$$B_i(t) = \binom{3}{i} t^i (1-t)^{3-i} \ , \ t \in [0,1] \ , \tag{4}$$

the choice approved by the known property of the Bernstein polynomials to be bounded over the unit interval, i.e. $0 \leq B_i(t) \leq 1$. Further, numerical computation of Bernstein polynomials is fast enough through de Casteljau algorithm [20]. It is considered an IFS with only two mappings $\{\mathbf{R}^2; \phi_1, \phi_2\}$, with two parameters, t_1 and t_2. In the tables below the coefficients of four different IFS's are given.

IFS1

a	b	c	d	e	f
$b_0(t_1)$	$-b_1(t_2)$	$b_2(t_1)$	$b_0(t_1)$	0.0	0.35
$b_0(t_2)$	$b_1(t_2)$	$-b_2(t_2)$	$b_0(t_2)$	0.6	0.1

IFS2

a	b	c	d	e	f
$b_0(t_1)$	$-b_1(t_2)$	$b_2(t_2)$	$b_0(t_1)$	0.0	0.45
$b_0(t_2)$	$b_1(t_1)$	$-b_2(t_1)$	$b_0(t_2)$	0.6	0.1

IFS3

a	b	c	d	e	f
$b_0(t_1)$	$-b_2(t_2)$	$b_2(t_2)$	$b_0(t_1)$	0.5	0.0
$b_0(t_2)$	$b_1(t_1)$	$-b_1(t_1)$	$b_0(t_2)$	2.5	1.5

IFS4

a	b	c	d	e	f
$b_0(t_1)$	$-b_1(t_1)$	$b_2(t_1)$	$b_0(t_1)$	0.0	0.55
$-b_0(t_2)$	$b_1(t_2)$	$-b_2(t_2)$	$b_0(t_2)$	0.4	0.1

As it can be seen from Figure 9, in spite of using only two contractions, exciting results are obtained. For the attractor *'feather'* (a) it was used IFS1, with parameters $t_1 = 0.1, t_2 = 0.22$. The *'cloud formation'* (b) uses IFS2 with $t_1 = 0.18, t_2 = 0.22$; Next three attractors are produced using IFS3: *'star'* (c) with $t_1 = 0.042, t_2 = 0.75$, *'Nautilus spiral'* (d) with $t_1 = 0.05, t_2 = 0.45$ and *'sunflower seed'* (e) with $t_1 = 0.033, t_2 = 0.52$. Finally, a *'fir twig'* (f) is formed by IFS4 with $t_1 = 0.09, t_2 = 0.18$.

Continuous variation of parameters t_1 and t_2 will reflect in continuous changing of the forms of attractors. In this way, it is possible to animate the sequence when the 'Nautilus spiral' transforms into 'sunflower' by running t_1 from 0.05 to 0.033, and t_2, from 0.45 to 0.52.

4. Modeling of natural phenomena

Describing a way of reproducing the wind, and a variety of natural forms by using parametric IFS, opens the question of using fractal sets in modeling

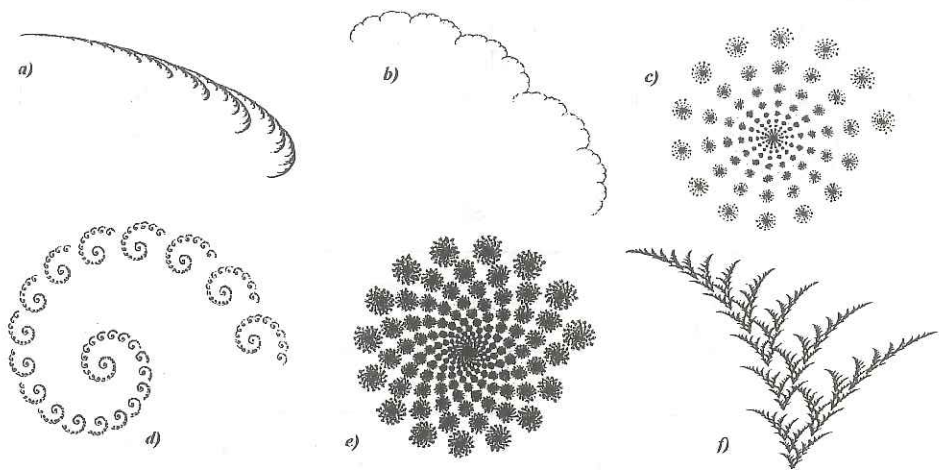

FIGURE 9. SIX ATTRACTORS GENERATED BY TWO-PARAMETER IFS CONTAINING BERNSTEIN POLYNOMIALS

wider class of forms and processes in the Universe. These forms are not easy to measure with classical Euclidean tools. So, a more sophisticated technique is developed. One of the important numbers associated with fractals is their Hausdorff dimension. The meaning of dimension is the 'density' with which the fractal set occupies the metric space in which it lies. It can be used for comparing fractals. It is an important parameter for modeling natural objects.

Definition 8. Let $K \in \mathcal{H}(\mathbf{X})$ be a nonempty set and $(\mathbf{X}, d)$ be a metric space. The *diameter* of K is

$$|K| = \sup_{x,y \in K} \{d(x,y)\} .$$

Definition 9. Let $\mathcal{K} = \{K_i\}_{i=0}^{+\infty}$ be a collection of sets in $\mathcal{H}(\mathbf{X})$ such that $0 < |K_i| \leq \varepsilon$, for each i. If $A \subset \cup_i K_i$, then $\mathcal{K}$ is ε-cover of A.

Definition 10. Let m be a positive integer and let A be a bounded subset of the metric space $(\mathbf{R}^m, d)$, where d is Euclidean metric. The function $p \mapsto \mu(A,p)$ defined as

$$\mu(A,p) = \sup_{\varepsilon > 0} \{\inf \{ \sum_{i=0}^{+\infty} |K_i|^p \}\} ,$$

where infimum is taken over all ε/covers of A, is called *Hausdorff p-dimensional measure* of A.

Definition 11. Let A be a bounded subset of the metric space $(\mathbf{R}^m, d)$. Then the real number $Dim_H(A)$ defined as

$$Dim_H(A) = \inf_{\mu(A,p)=0} \{p\},$$

is *Hausdorff dimension* of A. It is also called *Hausdorff–Besicovitch* or *geometrical dimension* of A.

Theorem 5. *Let A be a bounded subset of the space $(\mathbf{R}^m, d)$. $Dim_H(A)$ is a unique real number which satisfies $0 \leq Dim_H(A) \leq m$.*

Proof. See [1]. □

Hausdorff dimension of a typical fractal set may not be an integer number. This is 0.6309... for Cantor set, 1.2619... for von Koch curve, 1.5849... for Sierpinski gasket, 1.8927... for Sierpinski carpet or 2 for Peano curve. Fractal dimension may characterize type of relief and roughness of terrain or physical process. Hausdorff dimension of the coastline of Britain is ≈ 1.2 [18], while it is ≈ 1.5 for jet flame laboratory data [1]. It is possible to determine Hausdorff dimension of the chain of human DNA from genetic code [4], or for fractured metal surfaces [9]. Maybe painters or sculptors can be characterized by Hausdorff dimension of their masterpieces?

Practical determination of fractal dimension is not an easy task. It may depend on scaling. Mandelbrot gives an interesting example in [22] trying to answer to the question: 'What is the dimension of a ball of yarn?' From a great distance it is effectively a point, and appears zero dimensional; on approach it becomes a three-dimensional solid; moving closer discern the one-dimensional threads, which then become three dimensional again; the threads are again composed of fibers, etc. These different scaling regimes would produce rather extreme oscillations in a numerical estimate of dimension. Typically, when we are computing dimension we are interested in a given scaling range, but it may be very difficult to discern.

But there is a class of affine IFS whose attractors' dimension can be calculated without much trouble.

Definition 12. If the hyperbolic IFS $\{\mathbf{R}^m; \phi_i \; i = 1, \ldots, N\}$ has the following properties:

a) ϕ_i , $i = 1, \ldots, N$ are *similitudes*;

b) $\mu(\phi_i(B) \cap \phi_j(B)) = 0$, for $i \neq j$, and any $B \subset \mathbf{R}^m$,

then attractor A is *self-similar*.

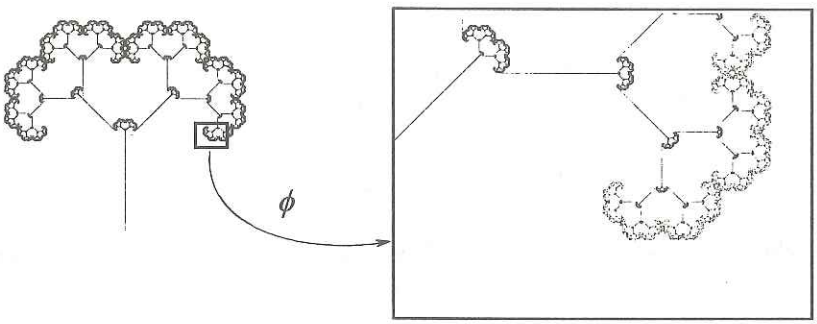

Figure 10. A self–similar set. Expanded area contains set that is identical to the whole set

Theorem 6. *Let A be self–similar attractor, generated by a hyperbolic IFS with s_i being a contractivity factor of ϕ_i. Then $D = Dim_H(A)$ is the unique solution of*

$$\sum_{i=1}^{N} |s_i|^D = 1, \quad D \in [0, m] .$$

Proof. See [1]. □

An example of self–similar fractal set is given in Figure 10. It means that a small portion of the set is identical to the whole set.

The property of self–similarity is important for modeling natural objects. Namely, natural scenes are organized in hierarchical structures. For example a forest is made of trees; a tree is a collection of boughs and limbs along a trunk; on each branch there are clusters of leaves; a leaf is filled with veins and covered with hairs. Similar hierarchy one can find in the structure of rocks, mountains, live forms... In every case, the object is built up from numerous near repetitions of some smaller structure. Although the natural entities have more complex kind of self–similarity, so called *statistical self–similarity*, the iterated function systems with similitudes
can be used for modeling approximations of such entities. Also, one can use some fractal set representing dynamics of some simple mapping, like the fractal set known as *Barnsley-3m*, being displayed in the left part of Figure 11. If specify the domain of mapping to be a rectangle denoted by 'A', the dynamical mapping will produce a magnified picture that resembles the 'wave' (right part of Fig. 11, above). Further multiplication reveals self–

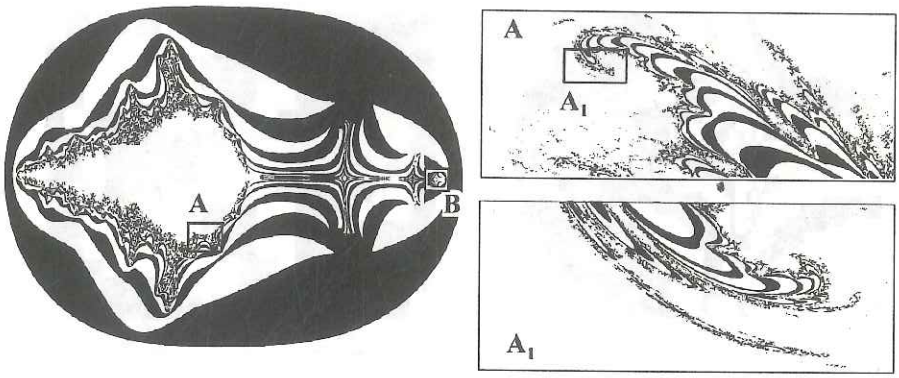

Figure 11. Fractal 'Barnsley-3m' and repeated magnification of its detail

similar structure of this fractal (Fig. 11, below). The fractal set 'Barnsley-3m' obtained by Barnsley [1] by applying the same principle as in the case of Mandelbrot set to more general functions of two complex variables. This set has connection with polarized-light microphotograph of some minerals. It reveals patterns that are less organic and more crystalline than those of the Mandelbrot and Julia sets. The dynamical system for 'Barnsley-3m' is given by

$$z_{n+1} = \begin{cases} Re^2 z_n - Im^2 z_n - 1 + i(2Re z_n Im z_n) , & Re z_n > 0 , \\ Re^2 z_n - Im^2 z_n - 1 + \lambda Re z_n + i(2Re z_n Im z_n + \lambda Re\, z_n) , & Re z_n \leq 0 , \end{cases}$$

where λ is a real parameter.

Besides self-similarity, the simplicity of IFS is the next attractive property of modeling natural scenes by fractals. It results in a tremendous compression of the data. Instead of keeping the whole picture in the computer's memory one can save only IFS code which gives compression ratio up to one hundred! To illustrate this, let us compare byte–length of an IFS file with that of the **pcx** format of the corresponding attractor picture: Barnsley fern 123 : 11732; von Koch curve 270 : 14368; Peano curve 586 : 25884 etc. For the **bmp** format the compression ratio is even larger.

Look at the fractal 'Barnsley-3m' from Figure 11. Computer–aided magnification of some part of the fractal set can be performed in two ways:

1. *By some graphical software;* The framed detail B is magnified using standard graphical package (for. ex. Corel-Draw). The result is shown in

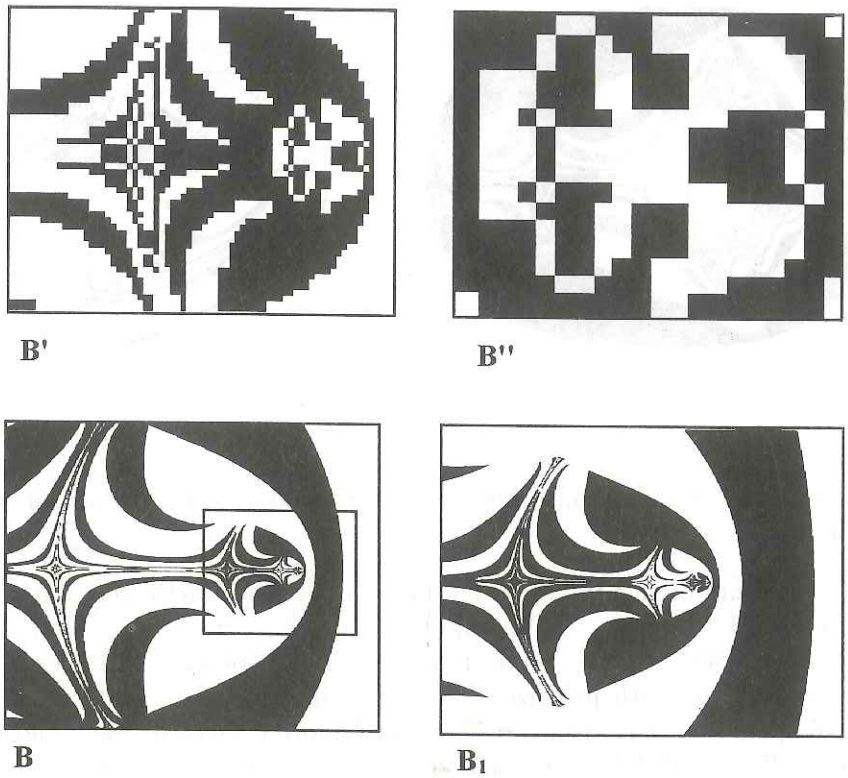

Figure 12. Magnification with or without loosing of details.

Figure 12, frame B'. Repeated magnification will cause further loosing of graphical information (frame B'').

2. *By fractal software;* If the same rule is used in the window B of *Barnsley3m* the picture framed by B in Figure 12 is produced. Repeated magnification of the frame B_1 is shown as the rightmost below frame. Fractal images can be magnified endlessly, without loosing of details.

So, fractal attractors are convenient for modeling different natural forms. Is it important to know how one can define an IFS to produce exactly the image that he wants? The answer is in the collage theorem:

Theorem 7 (Barnsley). *Let L be a nonempty compact subset of* X, *and*

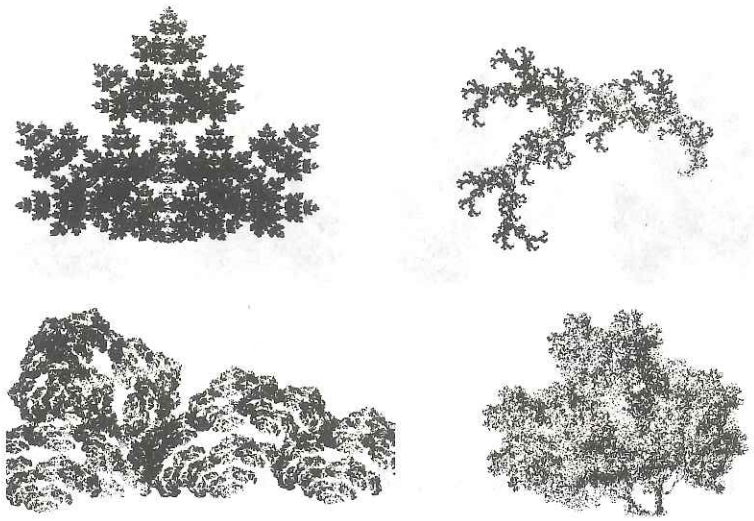

Figure 13. Fractals as natural forms: a leaf, a coral branch, rocks formation, and a tree crown

$\varepsilon \geq 0$ be given. Choose an IFS $\{\mathbf{X}; \phi_0, \ldots, \phi_N\}$ with contractivity factor $0 \leq s < 1$, so that $h(L, F(L)) \leq \varepsilon$, where $F(L) = \cup_{i=1}^{N} \phi_i(L)$, and $h(\cdot, \cdot)$ is Hausdorff metric. Then, $h(L, A) \leq \frac{\varepsilon}{1-s}$, where A is the attractor of the IFS.

Proof. See [1], [2] or [3]. □

The value of this theorem is in its practical side. It gives the procedure of constructing IFS, once the fractal attractor is given. Take, for example the leaf form in Figure 13. This is a subset in $(\mathbf{R}^2, d)$. Cover this figure by four smaller copies of this subset, as in making collage. Pieces do not fit quite perfect – some holes and overlappings will occur. These four copies are obtained by performing four affine contractions in $\mathbf{R}^2$: ϕ_1, ϕ_2, ϕ_3 and ϕ_4. This IFS is being used in generating the 'leaf' in Figure 13 by the random algorithm. The 'holes' in the leaf structure appear due to the holes in the collage. But, it is clear that the leaf form is obtained.

In the similar way the 'coral branch', ' formation of rocks' or 'tree crown' are obtained (Fig. 13).

Now, let say something about probabilities p_i that appear in Barnsley–Demko's random algorithm. Take the IFS $\{\mathbf{R}^2; \phi_1, \phi_2, \phi_3, \phi_4\}$ described above. The leaf image in Figure 13 is produced by the random algorithm

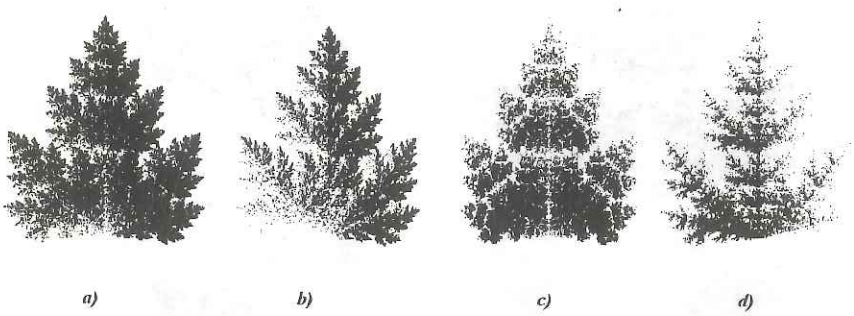

Figure 14. Leaves with different distribution of measure

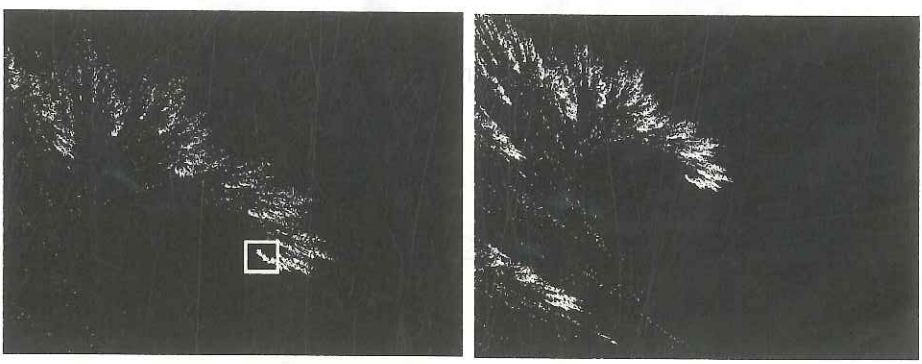

Figure 15. Waves from affine IFS

with uniformly distributed probabilities $(0.25, 0.25, 0.25, 0.25)$. If this vector changes into $(0.36, 0.16, 0.34, 0.34)$ the leaf a) in Figure 14 is obtained. Slight variation: $(0.46, 0.16, 0.34, 0.04)$ brings in an effect as though the leaf was lighted from the left (Fig. 14-b). The choice $(0.16, 0.16, 0.34, 0.34)$ will result into more rounded leaf (Fig. 14-c), while $(0.16, 0.56, 0.04, 0.04)$ gives a fir–tree (Fig. 14-d).

Phenomena in water, wrinkled surface, turbulences and streams can be nicely modeled by fractal sets. The magnifying details of *Barnsley3m* fractal

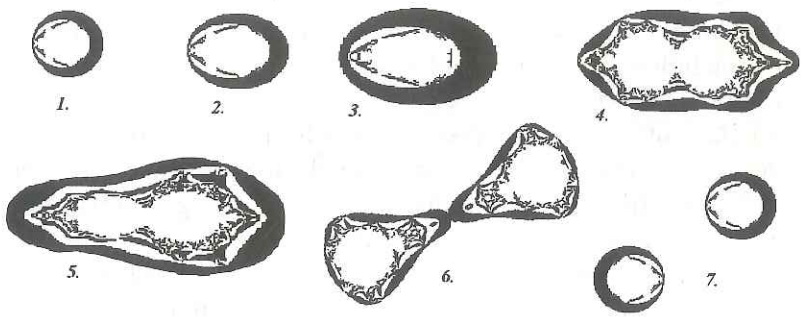

Figure 16. Modeling process of cell division

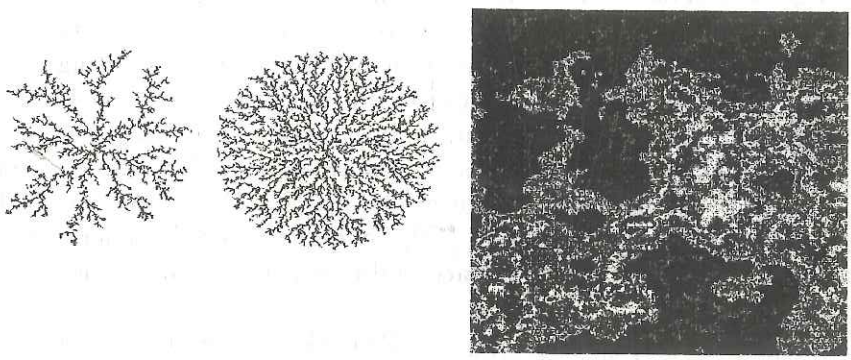

Figure 17. Crystal growth and a plasmatic cloud

from Figure 11 are good background for modeling waves. But they can be made using a simple affine IFS obtained by varying Takagi function (Fig 7-a). This 'wave' together with a magnification is shown in Figure 15.

The fractal, known from dynamical systems as *Mandellambda*, can be of help in modeling a biological process of cell division, Figure 16 (Stages are marked by numbers).

An important type of fractals are obtained by the physical processes known as diffusion–limited aggregation (DLA) [23]. This process is modeled by the use of random generator. Fractal forms obtained resembles tree root, and stand for models of growth of crystal structures (Figure 17).

If some fractal surface is intersected with a plane, a fractal level–line is obtained. These level–lines can be used to model clouds of different particles, which includes plasmatic cloud or intergalactic dust (see the rightmost illustration in Figure 17).

A large class of self–similar fractals are obtained by varying Peano and von Koch curves. The *Hilbert curve* , already mentioned in Section 1, has important application for digital halftoning. It has geometric dimension $Dim_H = 2$, the same as *Peano curve*, which means that it fills the square in the plane. An approximation of Hilbert curve is shown in Figure 18-a. Actually, all space filling curves are mappings $c : \mathbf{I} = [0, 1] \to \mathbf{R}^2$. The graph of c covers the square $\mathbf{I}^2$, so that it 'visits' all points of the square in ordered way if parameter t runs from 0 to 1. If $c_n : \mathbf{I} \to \mathbf{I}^2$ is an approximation of the space filling curve c. Subdivision of the interval $\mathbf{I}$ into n subintervals $\mathbf{I}_1, \ldots, \mathbf{I}_n$ will result in dividing square $\mathbf{I}^2$ into n subregions $R_1, \ldots, R_n$. The size of each subregion R_i varies proportionally with the length of the corresponding subinterval $\mathbf{I}_i$. The curve c_n visits all subregions R_i, actually each point of it. The restriction $c_i : \mathbf{I}_i \to \mathbf{R}_i$ is itself a space filling curve due to the self–similar property. Such restrictions will be used for selecting clusters of pixels (so called dithering) which results in different halftoning effects. This method of dithering using space filling fractal curves has an advantage over standard scan–image methods. Actually, it minimizes the grid effect, which results in better shadow textures [29]. Many variations of space filling curves include curves of Sierpinski [13], Lebesgue and Schoenberg [27] and others [21]. Two curves that fill space in different ways are shown in Figure 18-b and c.

This type of fractal curves inspired Prusinkiewitz and Lindenmayer to introduce L-systems for modeling plants and trees [25]. The central idea is that, in all cases, plants are defined by a small number of rules, applied repetitively to produce complex structures. L-system is a graph–rewriting mechanism, which operates on axial trees, and operates in parallel. The result is a fractal on graph alias *graftal.* Authors of [26] presented a model of tree synthesis which integrates botanical knowledge of the architecture of the trees.

5. Conclusion

This paper offers a short information on fractal geometry and its application in computer graphics and geometric modeling. This geometrz was born as a child of computer era, trying to explain some unsolved problems in mathematics, physics and related sciences. A great insight was given by the books of Mandelbrot [22] and Barnsley [1]. Fractals are sets having, in general, very complicated structure. The shortest definition of the class of

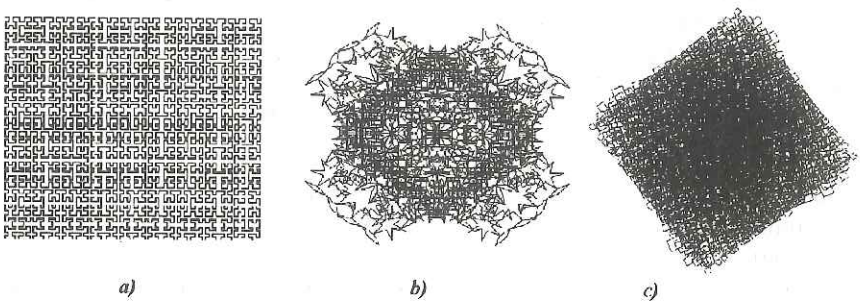

Figure 18. a) The Hilbert curve; b) and c) Two variations on Peano theme

so called *deterministic fractals* is that this is a subset of a compact metric space being invariant under the collection of contractive mappings. A simple but important example of such contractions are affine functions that map a plane into itself. This leads to the most important feature of deterministic fractals: self–similarity. Using this property, one can use fractal sets to model many natural forms having hierarchical self–similar structure: plants, rocks, water dynamics, clouds, foam, neural cells etc.

Text is illustrated with examples of fractal sets, together with some applications. All pictures, except Fig. 17, are produced by the software created by the author. Figure 17 was rendered by using the software *Fractint* by Bert Tyler.

References

[1] M. F. Barnsley, *Fractals Everywhere*, Academic Press, 1988.

[2] M. F. Barnsley, A. Jacquin, F. Malassenet, L. Reuter, A. D. Sloan, *Harnessing Chaos for Image Synthesis*, Comput. Graph. **22** (1988), 131–140.

[3] M. F. Barnsley, *Lecture Notes on Iterated Function Systems*, Chaos and Fractals. The Mathematics Behind the Computer Graphics (R. Devaney and L. Keen, eds.), Amer. Math. Soc., 1989, pp. 127–144.

[4] C. L. Berthelsen, J. A. Glazier, M. H. Skolnick, *Global fractal dimension of human DNA sequences treated as pseudorandom walks*, Phys. Rew. A **45** (1992), 8902–8913.

[5] B. Branner, *The Mandelbrot Set*, Chaos and Fractals. The Mathematics Behind the Computer Graphics (R. Devaney and L. Keen, eds.), Amer. Math. Soc., 1989, pp. 75–105.

[6] S. D. Casey, N. F. Reingold, *Self-Similar Fractal Sets: Theory and Procedure*, IEEE CG&A **14** (1994), 73–82.

[7] A. J. Cole, *Compaction Techniques for Raster Scan Graphics using Space-filling Curves*, Computer J. **30** (1987), 87–92.

[8] R. M. Corless, *Continued Fractions and Chaos*, Amer. Math. Monthly **99** (1992), 203–215.

[9] R. H. Dauskardt, F. Haubensak, R. O. Ritchie, *On the Interpretation of the Fractal Character of fracture surfaces*, Acta metall. **38** (1990), 143–159.

[10] S. Dubuc, A. Elqortobi, *Approximation of fractal sets*, J. Comput. Appl. Math. **29** (1990), 79–89.

[11] S. Eubank, D. Farmer, *An Introduction to Chaos and Randomness*, Lectures in Complex Systems, SFI Studies in the Sciences of Complexity (E. Jean, eds.), Addison-Wesley, 1990, pp. 75–190.

[12] B. R. Gelbaum, J. M. H. Olmsted, *Counterexamples in Analysis*, Mir, Moskva, 1967. (Russian)

[13] J. G. Griffiths, *Table-driven algorithms for generating space–filling curves*, Coput. Aided Design **17** (1985), 37–41.

[14] J. Harrison, *Continued Fractals and the Seifert Conjecture*, Bull. Amer. Math. Soc. **13** (1985), 147–153.

[15] J. Harrison, Chaos and Fractals. The Mathematics Behind the Computer Graphics (R. Devaney and L. Keen, eds.), Amer. Math. Soc., 1989, pp. 107–126.

[16] D. Hilbert, *Uber stetige Abbildung einer Linie auf ein Flächenstück*, Math. Annl. **38** (1891), 459–468.

[17] J. E. Hutchinson, *Fractals and Self Similarity*, Indian. J. Math **30** (1981), 713–747.

[18] J. Kappraff, *The Geometry of Coastlines: A Study in Fractals*, Comput. Math. Appl. **12B** (1986), 655–671.

[19] H. Von koch, *Sur une courbe continue sans tangente obtenue par une construction géométrique élémentaire*, Ark. Mat. Astr. Fys. **1** (1904), 681–704.

[20] LJ. M. Kocic, *Affine shape control of cubics*, PU.M.A. **3** (1992), 207–229.

[21] T. Lance, E. Thomas, *Arcs with Positive Measure and Space-Filling Curve*, Amer. Math. Monthly **98** (1991), 124–127.

[22] B. Mandelbrot, *The fractal geometry of nature*, Freeman, San Francisco, 1982.

[23] P. Meakin, J. Feder, T. Jøssang, *Radially biased diffusion–limited aggregation*, Physical Review A (1991), 1952–1964.

[24] G. Peano, *Sur une courbe, qui remplit toute une aire plane*, Math. Annl. **36** (1980), 157–160.

[25] P. Prusinkiewicz, A. Lindenmayer, J. Hanan, *Developmental Models of Herbaceous Plants for Computer Imagery Purposes*, Computer Graph. **22** (1988), 141–150.

[26] P. De Reffye, C. Edelin, J. Françon, M. Jaeger, C. Puech, *Plant Models Faithful to Botanical Structure and Development*, Computer Graph. **22** (1988), 151–158.

[27] H. Sagan, *Approximating Polygons for Lebesgue's and Schoenberg's Space Filling Curves*, Amer. Math. Monthly **93**, 361–368.

[28] T. Takagi, *A simple example of the continuous function without derivative*, Proc. Phys. Math. Soc. Japan **1** (1903), 176–177.

[29] L. Velho, J. M. Gomes, *Digital Halftoning with Space Filling Curves*, Computer Graph. **25** (1991), 81–90.

[30] M. T. Weiss, *An Early Introduction to Dynamics*, Amer. Math. Monthly **98** (1991), 635–641.

[31] S. WOLFRAM, *Geometry of Binomial Coefficients*, Amer. Math. Monthly **91** (1984), 566–570.

DEPARTMENT OF MATHEMATICS, FACULTY OF ELECTRONIC ENGINEERING, P.O.BOX 73, 18000 NIŠ